PERIDYNAMICS FOR FATIGUE DAMAGE PREDICTION IN NOTCHED COMPOSITES

Y. Hu[1], E. Madenci[2] and N. Phan[3]

[1]University of Arizona, Tucson, AZ 85721, USA
Email: yilehu@email.arizona.edu
[2]University of Arizona, Tucson, AZ 85721, USA
Email: madenci@email.arizona.edu
[3]Naval Air Systems Command (NAVAIR), Patuxent River, MD 20670, USA
Email: nam.phan@navy.mil

Keywords: peridynamics, fatigue, damage, composites

Abstract

Despite the development of many important concepts, the prediction of failure modes and strength of composite materials is still a challenge within the framework of the finite element method. This study presents a peridynamic modeling of laminated composites with arbitrary fiber orientation and stacking sequence in order to predict damage initiation and its growth under cyclic loading. Its capability is demonstrated by considering a unidirectional laminate with an edge crack under cyclic loading.

1. Introduction

It is a very challenging task to predict all possible failure modes (matrix cracking, fiber breakage, delamination) in composites because damage initiation and its progressive growth are very complex, and commonly accepted methods have had limited success. Aside from the complex loading conditions, the deformation of a laminate is dependent on the lamina properties, thickness, and stacking sequence.

Existing analysis methods face difficulties when predicting all possible failure modes in composites under multi-axial loading conditions and multiple-load paths. Silling [1, 2] introduced a nonlocal theory that does not require spatial derivatives, the peridynamic (PD) theory. This theory allows for damage in the material response. It is formulated by using integral equations, and this feature allows damage initiation and propagation at multiple sites, with arbitrary damage paths inside the material. Damage is inherently calculated without special procedures, making progressive failure analysis more practical.

In peridynamics, the internal forces are expressed through nonlocal interactions between the material points within a continuous body, and damage is part of the constitutive model. It effectively predicts complex failure modes in composites under general loading conditions. This study presents a PD approach for modeling composites with arbitrary fiber orientation and stacking sequence under cyclic loading. Its capability is demonstrated by considering a laminate with a pre-existing crack under cyclic loading.

2. Peridynamic laminate model

The PD theory [1, 2] concerns the physics of a material point that interacts with other material points within a certain range. The position of a material point in undeformed and deformed configurations

Excerpt from ISBN 978-3-00-053387-7

are denoted as $\mathbf{x}$ and $\mathbf{y}$, respectively. The interaction domain $H_{\mathbf{x}}$ of material point $\mathbf{x}$ is defined by its *horizon*, δ. Material points $\mathbf{x}'$, located within the domain $H_{\mathbf{x}}$ are called the *family members* of **x**. At any instant of time *t*, equilibrium between the acceleration term, internal force and external force must exist at each material point of a continuum given by

$$\rho\ddot{\mathbf{u}}(\mathbf{x},t)=\int_{H_{\mathbf{x}}}\mathbf{f}\left(\mathbf{u},\mathbf{u}',\mathbf{x},\mathbf{x}',t\right)dV_{\mathbf{x}'}+\mathbf{b}(\mathbf{x},t) \tag{1}$$

where ρ is the density of material, and $\mathbf{u}$, and $\mathbf{u}'$ are displacements of material points $\mathbf{x}$ and $\mathbf{x}'$, respectively. The volume of material point $\mathbf{x}'$ is denoted by $V_{\mathbf{x}'}$, and $\mathbf{b}$ is the force density vector. The pairwise force density vector, $\mathbf{f}$ arises from the interaction between material points $\mathbf{x}$ and $\mathbf{x}'$, and it is in opposite directions with equal magnitudes.

The present PD laminate model considers the interaction of material points within each ply as well as their interaction with other material points in the adjacent plies. The interactions are achieved through in-plane bonds and interlayer bonds as depicted in Fig. 1.

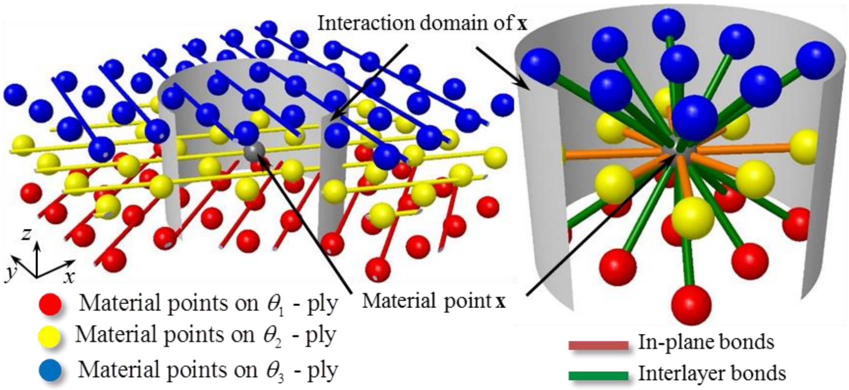

Figure 1. PD horizon for a material point **x** within a laminate

These bonds describe the nature of the deformation; thus, they can be associated with normal and shear deformations. Therefore, there exist four types of bonds: in-plane normal and shear bonds, and interlayer (transverse) normal and shear bonds. The in-plane normal and shear bonds are not the same as fiber and matrix bonds introduced in the previous PD composite models [3-7]. The kinematics and force density relations are described in detail by Hu and Madenci [8] without any constraints on the engineering material constants.

3. Damage prediction

When the stretch between two material points exceeds a critical value, the interaction is permanently removed, and the interaction forces vanish through a status (Heaviside step) function, $\mu(\mathbf{x},\mathbf{x}',t)$. The material point **x** has in-plane interactions within the same ply, as well as interlayer interactions between the adjacent plies above and below. The local damage at a material point **x** is defined as the ratio of the number of the broken interactions to the total number of interactions within the horizon $H_{\mathbf{x}}$, given by

$$\varphi(\mathbf{x},t)=1-\frac{\int_{H\mathbf{x}}\mu(\mathbf{x},\mathbf{x}',t)dV'}{\int_{H\mathbf{x}}dV'} \tag{2}$$

Excerpt from ISBN 978-3-00-053387-7

The local damage ranges from zero to one. When the local damage is one, all the interactions initially associated with the point have been eliminated, while a local damage of zero means that all interactions are intact. The measure of local damage is an indicator of crack formation within a body. The details of the failure criteria and local damage are given by Hu et al. [9].

The number of cycles to crack initiation N_D can be obtained from the experimental crack initiation data which can be expressed in the form of a power law as

$$N_D = \left(\frac{1}{m_1}\right)^{\frac{1}{m_2}} G^{\frac{1}{m_2}} \tag{3}$$

where G is the energy release rate at the crack tip, and the parameters $m_1 = 0.2023$ and $m_2 = -0.078924$ are obtained from the published data [10, 11]. Matrix cracking may occur due to opening mode (mode I) or shearing mode (mode II) when the energy release rate reaches its critical value. Therefore, the PD energy release rate for these deformation states between material points $\mathbf{x}_{(i)}$ and $\mathbf{x}_{(j)}$ is calculated as

$$G_I^{(i)(j)} = \frac{\int \left(f_{y(i)(j)} V_{(i)} V_{(j)} \right) dv_{(i)(j)}}{h\Delta y} \quad \text{and} \quad G_{II}^{(i)(j)} = \frac{\int \left(f_{x(i)(j)} V_{(i)} V_{(j)} \right) du_{(i)(j)}}{h\Delta x} \tag{4}$$

where $f_{x(i)(j)}$ and $f_{y(i)(j)}$ are the force density components, and $u_{(i)(j)}$ and $v_{(i)(j)}$ are displacement components of the bond between these material points with incremental volumes, $V_{(i)} = V_{(j)}$. The parameter $\Delta x = \Delta y$ is the uniform spacing between these points, and h is the thickness of a laminate.

After the initiation stage, the crack grows in a stable manner according to the Paris-Erdogan law as

$$\frac{da}{dN} = c \cdot G^n \tag{5}$$

where da/dN is the increase in crack length per cycle, and G is the energy release rate at the peak loading during one cycle. The factor c and exponent n are obtained from the experimental data [10, 11], their values are $c = 2.44 \times 10^6$ and $n = 10.61$. When the energy release rate G at crack tip becomes lower than the threshold value G_{th} crack growth is terminated.

Crack growth rate is assumed to be constant within one grid spacing Δx; therefore, the number of cycles for stable crack growth is expressed as

$$\Delta N_k = \frac{\Delta x}{c \cdot G_k^n} \tag{6}$$

Thus, the number of cycles during stable crack growth can be calculated in the form

$$N_G = \sum_{k=1}^{K} \Delta N_k \tag{7}$$

Excerpt from ISBN 978-3-00-053387-7

where K is the total number of increments, and crack length is obtained by adding the incremental lengths Δx to the initial length a_0 as

$$a = a_0 + K\Delta x \tag{8}$$

Consequently, the total life N_T of a structure under fatigue loading is given by

$$N_T = N_D + N_G \tag{9}$$

4. Numerical procedure

Under a quasi-static loading condition, the inertial term on the left of Eq. (1) is zero. Therefore, the PD equilibrium equation can be expressed as

$$\mathbf{L}(\mathbf{u}) + \mathbf{b} = \mathbf{0} \tag{10}$$

where the internal force density is defined by an integral operator $\mathbf{L}(\mathbf{u})$. The tangent stiffness matrix is obtained as

$$\mathbf{K}_\mathrm{T} = \frac{\partial \mathbf{L}}{\partial \mathbf{u}} \tag{11}$$

in which $\mathbf{L}(\mathbf{u})$ is the internal force density vector in terms of the displacement vector, $\mathbf{u}$. As part of the analysis, the incremental equilibrium equations can be expressed in a recursive form

$$\mathbf{K}_\mathrm{T}^n \Delta\mathbf{u}^{n+1} = \Delta\mathbf{b}^{n+1} \tag{12}$$

where $\mathbf{K}_\mathrm{T}^n = \mathbf{K}_\mathrm{T}(\mathbf{u}^n)$, $\Delta\mathbf{u}^{n+1} = \mathbf{u}^{n+1} - \mathbf{u}^n$, $\Delta\mathbf{b}^{n+1} = \mathbf{b}^{n+1} - \mathbf{b}^n$ and $n = 0,1,2,......,N$. At each incremental step, the tangent stiffness matrix is obtained from previously known state $\mathbf{u}^n$, and it is used to solve for the next unknown state $\mathbf{u}^{n+1}$. The system of equations is solved by the Generalized Minimal Residual algorithm.

5. Numerical results

A square laminate is subjected to cyclic tensile loading applied at two corners as shown in Fig. 2. The laminate has dimensions of $L = W = 100$ mm and thickness $h = 1$ mm. It is made of T300/1076 unidirectional graphite/epoxy prepreg with elastic properties are specified as $E_L = 139.4$ GPa, $E_T = 10.6$ GPa, $G_{LT} = 4.6$ GPa, and $\nu_{LT} = 0.3$, and its mode I critical energy release rate is $G_{Ic} = 0.1703$ kJ/m^2. The threshold value is specified as $G_\mathrm{th} = 0.06$ kJ/m^2 [10, 11]. The loading is achieved by applying displacement constraints at the upper- and lower-left corners. It is varied between $v_{\max}$ and zero. The maximum applied displacement $v_{\max}$ is determined based the PD calculations for an initial crack length of $a_0 = 40$ mm while invoking the assumption of $G_{I\max} = 0.8G_{Ic}$. With this assumption, Eq. (3) yields the number of cycles for crack initiation as $N_D = 149$. After discretizing the laminate with a computational grid of 200×200 with $\Delta x = 0.1$ mm, the energy release rate at the crack tip is calculated for eleven different initial crack length values that

Excerpt from ISBN 978-3-00-053387-7

vary between $40\text{mm} \le a_0 \le 60\text{mm}$. With these PD calculations, the energy release rate expression can be constructed as a function of initial crack length in the form

$$G(a_0) = 1.739\times10^{-7} a_0^3 - 3.533\times10^{-5} a_0^2 - 1.2386\times10^{-4} a_0 + 0.1866 \tag{13}$$

After substituting for the energy relase rate in Eq. (5), its integration yields the theoretical number of cycles N_G for stable crack growth. The resulting relation between crack length and number of cycles is shown in Fig. 3 as the theoretical benchmark (solid red curve).

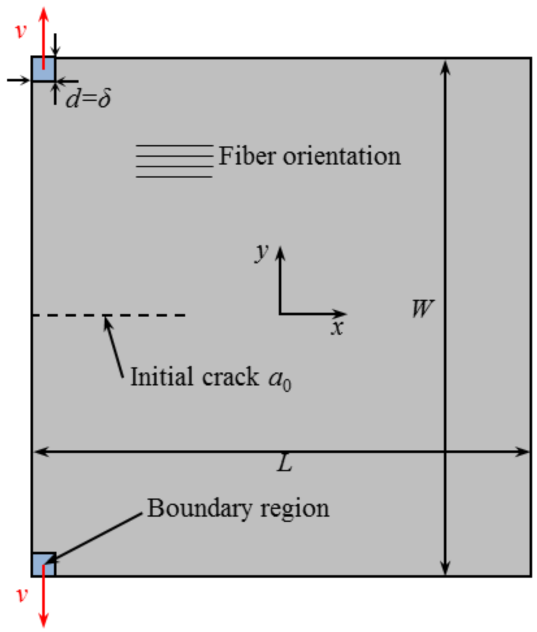

Figure 2. A square laminate with a pre-existing crack under cyclic loading at the corners.

Also, PD analysis is performed under constant amplitude loading for specified initial crack length of $a_0 = 40$ mm with varying discretizations of 100×100, 150×150 and 200×200. Based on the computed values of energy release rate, G at the crack tip, the number cycles, ΔN necessary to grow the crack by an amount of Δx is computed by using Eq. (6). Figure 8 shows the predicted relation between the crack length and the number of cycles; the prediction obtained with 200×200 discretization has a very good agreement with theoretical benchmark. When the energy release rate, G at crack tip becomes lower than the threshold value G_{th}, crack growth is terminated. In all cases, crack propagation stops when number of cycles is about 10^7; therefore, the numerical models with different grid spacing converges to the sam e prediction of total number of cycles. Figure 9 presents the PD prediction of crack growth rate. The numerical estimates of factor c and exponent n are determined based on the PD calculations. The PD approach is able to recover the theoretical crack growth rate. Figure 10 presents the crack propagation process from the PD analysis; deformations are exaggerated for a more clear visualization. The four images on top show the displacement field in the y-direction at different crack length. Discontinuities due to the existence of crack can be observed. The four image below are damage patterns when crack length reaches to $a = 40,\ 50,\ 60$ and 70 mm, respectively.

Excerpt from ISBN 978-3-00-053387-7

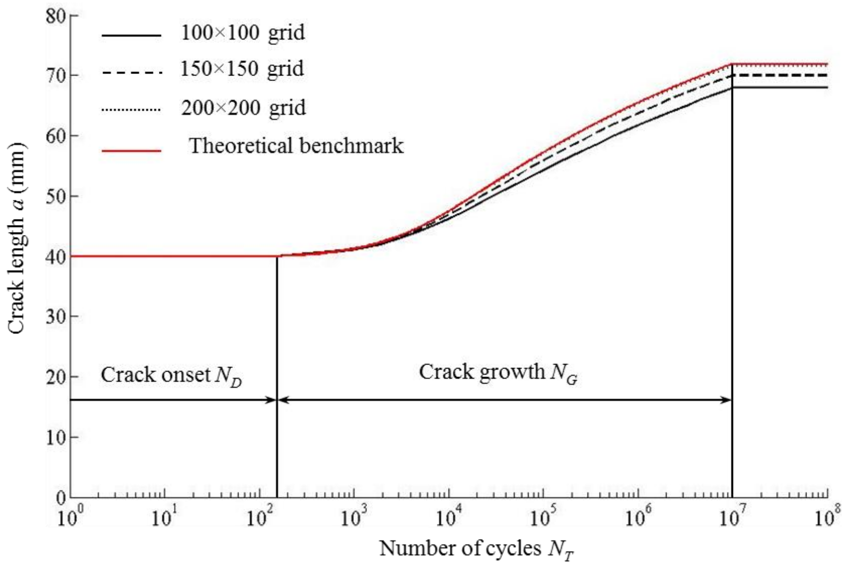

Figure 3. Peridynamic predictions of the relation between crack length and cycle number.

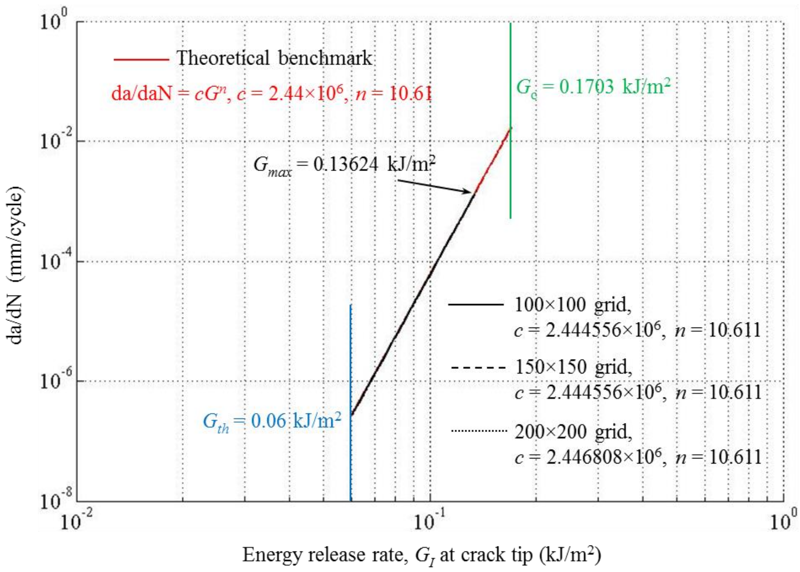

Figure 4. Comparison of crack growth rate between theoretical value and PD predictions

Excerpt from ISBN 978-3-00-053387-7

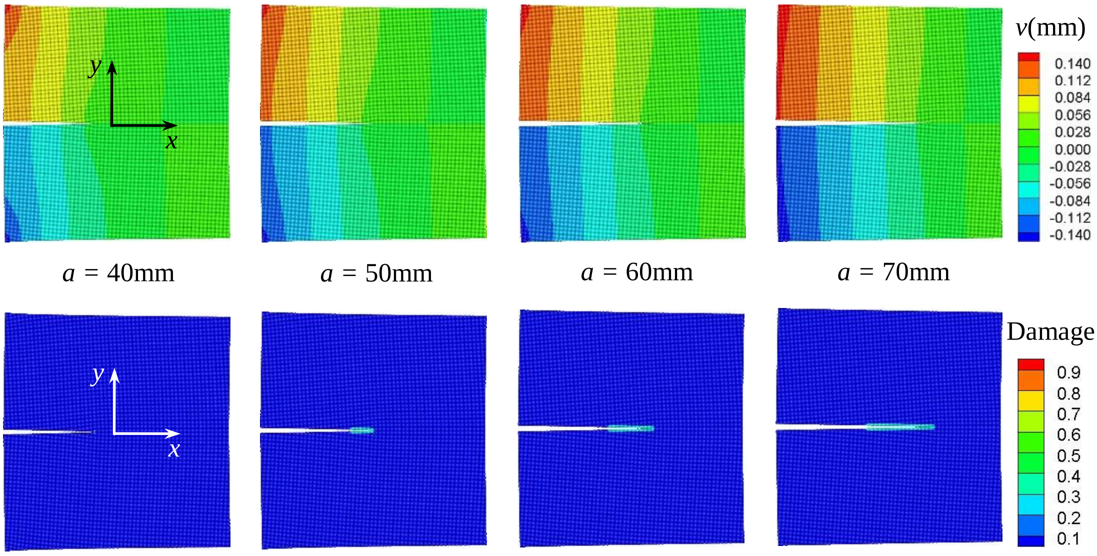

Figure 5. Peridynamic simulation of crack propagation under cyclic loading.

6. Conclusions

This study presents a peridynamic (PD) modeling of laminates under cyclic loading. It relies on the experimental fatigue data for a lamina along with the critical energy release rate. The PD calculations recover the expected theoretical crack growth rate, and the material constants that appear in the expression for the crack growth rate.

References

[1] Silling, S.A., (2000) *J. Mech. Phys. Solids* **48**, 175-209.
[2] Silling, S.A., Epton, M., Weckner, O., Xu, J. and Askari, A. (2007) *J. Elast.* **88**, 151-184.
[3] Hu, W., Ha. Y. D. and Bobaru, F. (2011) *Inter. J. for Multiscale Computational Engineering* **9**, 707–726.
[4] Oterkus, E. and Madenci, E. (2012) *J. of Mechanics of Materials and Structures*, **7**, 45-84.
[5] Kilic, B., Agwai, A. and Madenci, E. (2009) *Composite Structures* **90**, 141-151.
[6] Hu, Y. L., Yu, Y. and Wang, H. (2014) *Composite Structures* **108**, 801-810.
[7] Madenci, E. and Oterkus. E. (2014) Peridynamic Theory and Its Applications, *Springer*, Boston, MA.
[8] Hu Y.L. and Madenci, E. (2016) *Composite Structures*, (submitted).
[9] Hu Y.L., De Carvalho, N.V. and Madenci, E. (2015) *Composite Structures* **32**, 610-620.
[10] Krueger, R. (2010) *NASA/CR-2010-216723*, NIA report No. 2010-04.
[11] Krueger, R. (2012) *Simulia Community Conference*.

Excerpt from ISBN 978-3-00-053387-7